Linewidth determination in local oxidation nanolithography of silicon surfaces

Marta Tello, Fernando García, and Ricardo García[a)]
Instituto de Microelectrónica de Madrid, CSIC Isaac Newton 8, 28760 Tres Cantos, Madrid, Spain

(Received 1 April 2002; accepted for publication 28 June 2002)

We measure the linewidth of structures fabricated by local oxidation lithography on silicon surfaces. Two different structures, isolated and arrays of parallel lines have been generated. The oxide structures have been fabricated in the proximity of sexithiophene islands whose size is comparable to the oxide motives. The comparison between local oxides and sexithiophene islands reveals that atomic force microscopy (AFM) images faithfully reproduce the size and shape of local silicon oxides. The oxide lines have a trapezoidal shape with a flat section at the top. AFM images of the oxide structures show rather small slopes $\sim 0.05-0.15$ which imply angles with the horizontal between 3° and 8°. The shallow angles imply a minimum feature size of 14 nm at the base for an oxide thickness of 1 nm. Linewidths of 7 nm and 20 nm at the top and base, respectively, have been fabricated. We have also demonstrated the ability to pack structures with a periodicity of 13 nm. © *2002 American Institute of Physics.* [DOI: 10.1063/1.1501753]

I. INTRODUCTION

Nano-oxidation or local oxidation of semiconductor and metallic surfaces by atomic force microscopy (AFM) is emerging as a reliable and versatile lithographic method for fabrication of devices and patterning of structures at nanometer scale.[1–4] A variety of materials have been locally oxidized such as silicon,[5] silicon nitride,[6] GaAs,[7] titanium,[8] niobium,[9] aluminum,[10] carbonaceous films,[11] and organic monolayers.[12]

The strong activity devoted to this lithography has allowed us to identify the relevant factors affecting the oxidation process. Among the key factors controlling the oxide growth are the production of charged defects within the oxide,[5] the formation of a liquid bridge,[4] the voltage and pulse duration,[13,14] and the cantilever force constant.[15] The present knowledge allows us to establish some similarities to conventional anodic oxidation. The AFM tip is used as a cathode and the water meniscus formed between tip and surface is the electrolyte. The strong localization of the electrical field lines near the tip apex gives rise to a nanometer-size oxide dot.

In parallel to fundamental studies,[4,5,14–16] several nanometer-scale devices such as single electron[3] and metal–oxide[1] transistors, quantum wires,[2] high density memories,[4,17] and Josephson junctions[18] have illustrated some of the nanoelectronic applications. Machining of silicon structures has also been demonstrated by AFM oxidation.[19] Furthermore, local oxidation lithography is compatible with the operation of parallel tip arrays.[20] This opens the possibility to pattern cm^2 surfaces with nanometer-size motives.

In view of the range of device applications, it is surprising to realize that few contributions, if any, have been devoted to study the minimum feature size obtained by local oxidation lithography. Nonetheless, sub-10 nm feature sizes have been claimed several times. Garcia *et al.*[4] have fabricated arrays of thousands of dots with a periodicity of 40 nm. Image reconstruction of individual dots allowed them to estimate the width of the dot in the 5–15 nm range. Cooper *et al.*[17] have used single-wall carbon nanotube tips to generate arrays of dots with a periodicity of 20 nm on titanium surfaces. That result suggests a dot size below 20 nm. Gotoh *et al.*[21] have fabricated two parallel lines on titanium surfaces. A cross section revealed a triangular shape with a linewidth of 7 nm at half maximum. These results definitely illustrate some sub-10 nm potential, however, in many cases the measurements were obtained directly from AFM images with no or little consideration for the influence of the tip on the measurements. For example, our previous results[4] were based on an image reconstruction process that involved spherical tips of 51 nm of radius. Those values were obtained by calibrating the tip with semiconductor dots of about 10 nm in height, i.e., several times higher than the oxide structures. Because the nonlinear character of the imaging process in AFM, it seems questionable to extrapolate tip radius values obtained by calibrating the tip with structures of different sizes.

The definition of lateral resolution in AFM is, in itself, a delicate issue because the nonlinear character of the imaging process. Furthermore, due to the finite tip size, an AFM image is a combination of the shape of the probe and the shape of the object. This implies that to obtain faithful lateral measurements, the AFM image should be reconstructed which implies the determination of the tip geometry. This is certainly a sophisticated and time consuming process. To simplify things, we have opted to fabricate the structures in the proximity of an object of known shape.

Here, we explore the feature size of local oxides on silicon surfaces imaged by AFM. We have chosen to generate single, and arrays of, oxide lines. On the one hand, lines

[a)]Author to whom all correspondence should be addressed; electronic mail: rgarcia@imm.cnm.csic.es

require a sequential oxidation process which in turns implies more general results. On the other hand, lines are more representative of the kind of elements needed to fabricate devices by local oxidation lithography.

The article is organized as follows. In Sec. II, the experimental details are described. The fabrication and measurement of single lines are described in Sec. III. Section IV addresses the potential of local oxidation to fabricate sets of parallel lines. Finally, in Sec. V, a discussion and the main conclusions of this contribution are summarized.

II. EXPERIMENTS

The experiments are performed with an AFM operated in noncontact mode. The microscope was equipped with additional circuits and power supply to perform the oxidation. Silicon cantilevers, $n+$ doped with a resistivity in the 0.01–0.025 Ω cm range (Nanosensors, Germany) were used. The average force constant (k_c) and resonance frequency (f_0) were about 34 N/m and 300 kHz, respectively. The samples were p-type Si(100) with a resistivity of 15 Ω cm. For environmental control, the microscope was placed into a closed box with inlets for dry and H_2O saturated nitrogen. Due to exposure to air, the silicon surface has a native oxide layer of about 2 nm. However, the native oxide does not interfere with local oxidation processes.

Amplitude modulation AFM operation conditions were determined by recording amplitude and phase versus distance curves. In all cases, a set point amplitude value belonging to the low oscillation branch was chosen (noncontact operation). Theoretical as well as experimental details about amplitude modulation AFM operation can be found elsewhere.[22,23]

Several parameters control feature size in noncontact AFM oxidation such as meniscus diameter, pulse duration, and voltage strength. Meniscus size is controlled by the tip geometry, electrical field, and tip–surface separation. We have chosen a combination of relative high voltages and short pulses to generate the oxides as a means to optimize their aspect ratio.[14]

Our protocol distinguishes two different uses of the AFM, imaging, and modification. Toward that purpose, we have used silicon samples with photolithography markers. Those markers allow the positioning of the tip in a selected region of the sample. To minimize the convolution effects of the tip, we have used several tips for the topographic characterization of the local oxides. The tips have been selected by imaging gold colloidal particles of 8 nm in diameter. From those measurements, we inferred that the tips used here have a curvature radius between 12 to 25 nm. Furthermore, the tips have been recalibrated by imaging sexithiophene molecules (6T) placed close to the oxide structures. Under certain conditions, those molecules form monolayer islands of 2.4 to 3 nm in height.[25]

In this contribution, we have measured the linewidths of isolated and interdigitated lines. Isolated lines allow us to determine the absolute value of the local oxide feature size, while the fabrication of interdigitated lines provide a procedure to discuss the ability of local oxidation nanolithography

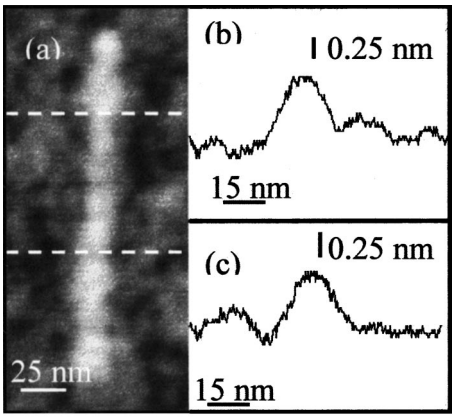

FIG. 1. (a) AFM image of a single silicon oxide line. (b) and (c) cross sections along the dashed lines shown in (a). The line was generated by applying a succession of pulses of 24.7 V and 80 μs.

to integrate features in a device. We have fabricated single oxide lines of 200 nm in length. To measure its width, images of 150 nm with 512 acquisition data points were taken. That means a pixel size of 0.3 nm. Each line is generated by applying a sequence of voltage pulses. Between pulses the tip is laterally displaced 3.5 nm.

III. LINEWIDTH OF SINGLE LINES

Figure 1 shows an AFM image of a single oxide line of 200 nm in length. To fabricate such a line, a sequence of 57 pulses of 24.7 V and 80 μs were applied. This line is representative of the sharpest lines obtained with the present protocol. The sample roughness and/or small tip–surface separation changes during the oxidation could be the responsible for the slight width variations observed along the line [see Fig. 1(a)]. The cross section reveals a trapezoidal shape with a flat region on top between 7 and 10 nm and a baseline ranging between 20 and 26 nm. The slope of the line (height/width) ranges between 0.05 and 0.12. It depends on the actual cross section chosen. These values come directly from unreconstructed AFM images. The question arises to which degree those values represent the *real* oxide features.

Several procedures have been suggested to reconstruct AFM images, however, all of them require the determination of the tip shape.[24] To determine whether or not the tip shape introduces a distortion in the images of local oxide structures, we have fabricated lines close to sexithiophene (6T) islands. Those islands have vertical sidewalls with a lateral variation estimated in 0.5 nm, i.e., they could be considered as perfectly vertical when the lateral scale involves tens of nanometers.

Figure 2 shows a cross section of two oxide lines in the

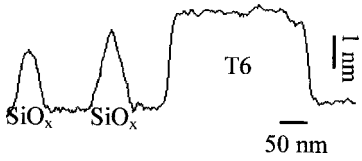

FIG. 2. Cross section along two oxide lines fabricated in the proximity of a 6T monolayer island.

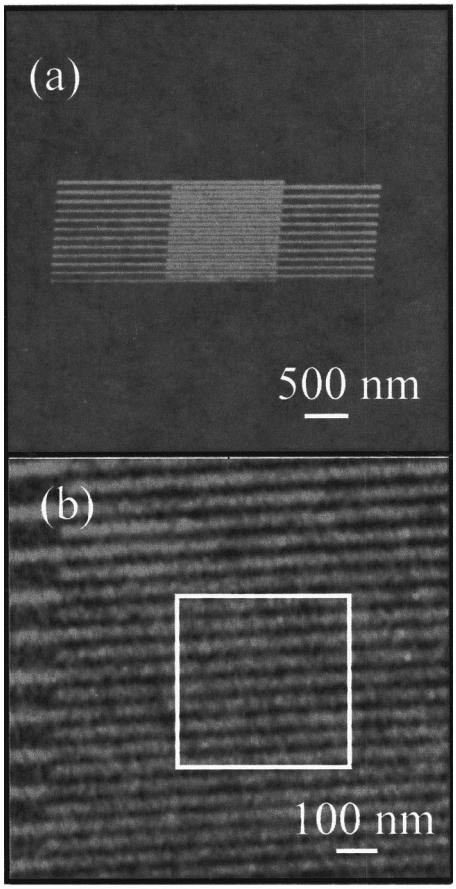

FIG. 3. AFM images of a set of 23 interdigitated lines placed 43 nm apart. (a) Full view of the structure. (b) Interdigitated area. The lines were obtained by applying a sequence of pulses of 21 V for 1 ms.

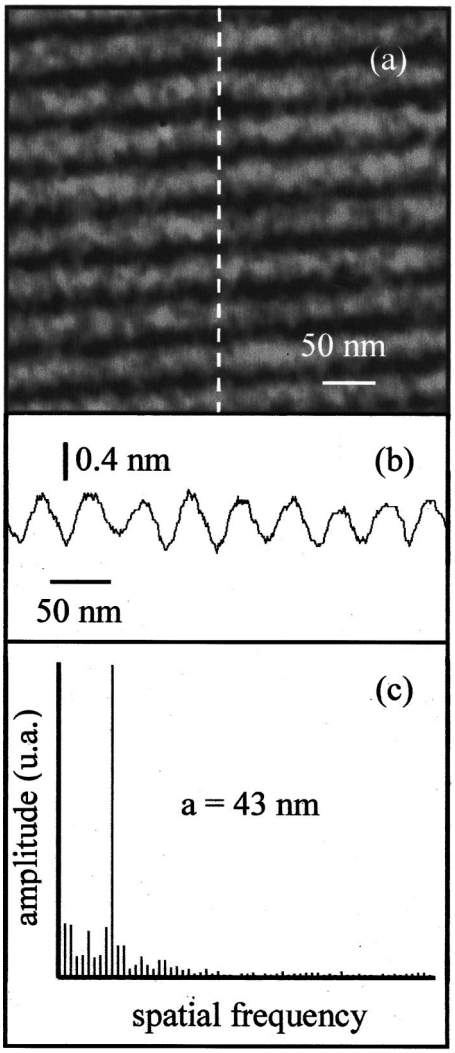

FIG. 4. High-resolution image of the area marked in Fig. 3(b). (b) Cross section along the dashed line of (a). (c) Spatial spectrum. The sharp peak at 43 nm illustrates the strong spatial periodicity.

vicinity of a 6T monolayer island. The average slope of the lines is 0.09, i.e., very close to previous values. However, the monolayer island shows an average slope of 0.23, i.e., about a factor 2.5 higher than the one corresponding to the oxide. Because the lines and 6T monolayer have similar heights, 2.4 versus 3 nm, respectively, the values measured in the oxide structures could not be attributed to any tip–sample convolution effect. Consequently, we conclude that unreconstructed AFM images of the oxide lines reflect their *real* lateral values.

IV. INTERDIGITATED LINES

To determine the potential of local oxidation lithography to integrate devices and connections, we have measured the linedwidth of interdigitated lines. Figure 3(a) shows a set of 23 interdigitated lines. Each line has been obtained by applying a sequence of 285 pulses of 21 V for 1 ms. The lines are slightly shifted toward the right-hand side of the image. This is due to the creep of the $x-y$ scanner. A closeup of the interdigitated area shows the line edges and their interspacings [Fig. 3(b)].

Figure 4(a) shows a high-resolution image of the central region marked in Fig. 3(b). The cross section shows the sequence of peaks and valleys of the parallel array [Fig. 4(b)]. The average slope obtained from the image is 0.04, i.e., slightly smaller than the values measured in isolated lines. On the other hand, the spatial spectrum shows a sharp peak at 43 nm.

Similar results can be obtained by halving the line spacing. Figure 5(a) shows an AFM image of 18 interdigitated lines. Each line has been obtained by applying a sequence of 87 pulses of 21 V for 80 μs. Between pulses, the tip is laterally displaced 3.5 nm. The average slope is of 0.08. The spatial spectrum of the cross section shown in Fig. 5(b) has a dominant and sharp peak at 19.5 nm [Fig. 5(c)]. The dominance of the 19.5 nm peak demonstrates the reliability of local oxidation to pattern sub-20 nm motives.

A higher packing density has been achieved by writing a set of 19 lines with a separation of 13 nm (Fig. 6). Each line has been obtained by applying a sequence of pulses of 24.7 V for 80 μs. The lines are hardly resolved in the AFM image, although clearly visible in the average cross section [Fig. 6(b)]. The average slope is of 0.1 in this case.

V. DISCUSSION AND CONCLUSIONS

There is not yet an accepted definition on the pattern or structure more convenient to determine the minimum feature

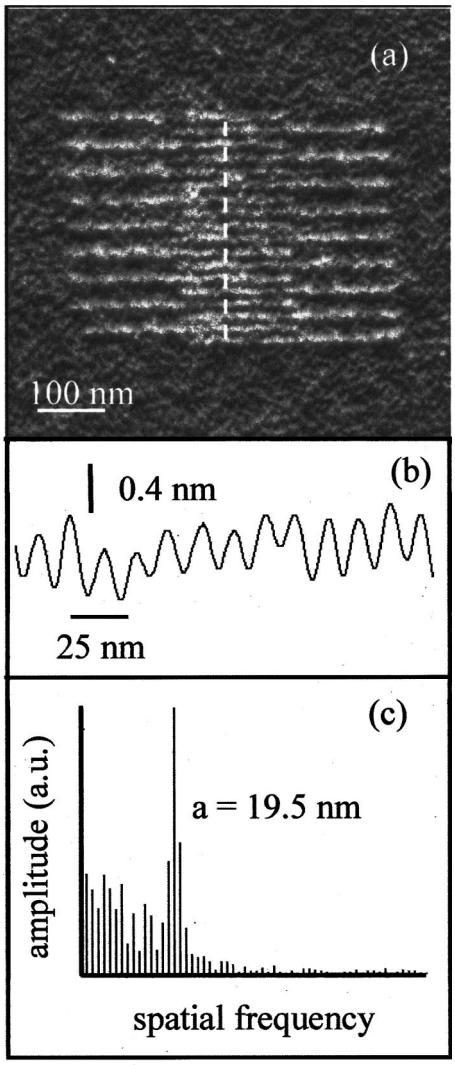

FIG. 5. (a) AFM image of a set of 18 interdigitated lines. (b) Cross section along the dashed line in (a). (b) The Fourier transform of (b) reveals a periodicity of 19.5 nm. The lines were obtained by applying pulses of 21 V and 80 μs.

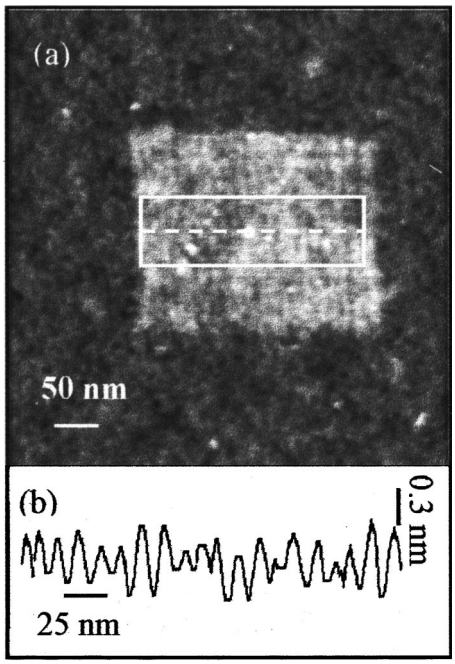

FIG. 6. (a) AFM image of a set of 19 parallel lines placed 13 nm apart. (b) The cross section reveals a spatial periodicity of 13 nm. The lines were obtained by applying a sequence of pulses of 24.7 V and 80 μs.

size obtained by local oxidation nanolithography. Some authors have fabricated single or array of dots to determine feature sizes. Here, we have chosen lines because they are more representative of the kind of motives needed for device applications. In general, to deduce the minimum feature size of a patterned structure involves several steps. First, to estimate the tip curvature radius and, second, to reconstruct the object shape from the AFM image and the tip geometry.

To determine the size and shape of the oxide lines as well as to estimate the distortion introduced by the tip in the AFM image, we have fabricated some oxide lines close to molecules (6T) of well defined side walls and with heights similar to the oxide lines. The side walls of 6T molecules can be considered vertical except for the incertitude of the lateral extension of the molecular orbitals. We assume a higher limit for the lateral extension of 0.5 nm.

Figure 2 shows that the slope of 6T islands is higher than those of the oxide lines by a factor 2.5, $\sim$0.23 versus 0.09, respectively. The difference observed between the slope of the 6T molecule and its ideal value ($\sim$50) allows one to deduce a curvature radius of the tip of 12 nm. The deduction uses exclusively geometrical arguments. It does not consider the long-range character of interaction forces in noncontact AFM. Nonetheless, such a difference allow us to conclude that unreconstructed AFM images of oxide lines provide a faithful description of their shape and size. This is further supported by the observation that, in some cases, the slope of the lines is not uniform. Sharper sections are observed, for example, in Fig. 1(c). In general, the cross section reveals trapezoidal shape with a flat section at the top. This conclusion is further supported by measurement of the slopes of hundreds of oxide lines and dots taken over a period of two years. More than 20 tips have been used in the process. In all cases, the slopes belong to the 0.05–0.15 interval. From the slope measurements, we deduce that the angle of the oxide structure and flat substrate is between 3° and 8°. Those values impose, for an oxide height of 1 nm, a minimum feature size at the baseline of 14 nm. The trapezoidal shapes and slope values deduced from AFM images are, on the other hand, consistent with cross-sectional electron microscopy images of local oxides obtained by operating the AFM in contact mode and by using oxidation times about two order of magnitude longer.[26–27] From Morimoto *et al.*,[27] the electron microscope pictures, show a slope of about 0.07 can be obtained for a local oxide of 3.9 and 225 nm in height and width, respectively. The slope values obtained from electron microscopy images are within the range determined from AFM images.

Figure 7 points out the limitations of AFM measurements at half height [full width at half maximum (FWHM)] to describe packed structures. The proximity of the structures and tip–line convolution effects prevent the tip from reaching the substrate. As a consequence, the apparent height of

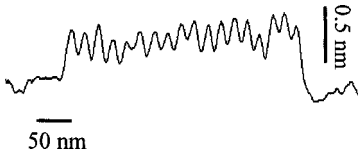

FIG. 7. Cross section along the dashed line of Fig. 5(a). The cross section is extended beyond the patterned area to include the bare substrate.

the lines is smaller than its real height which in turns gives a smaller FWHM. The height difference between peaks and valleys inside the pattern is about 0.3 nm; while between the peaks and the flat substrate outside the pattern, the difference is about 0.7 nm. This, in turn, may produce smaller FWHM values for parallel arrays. For instance, FWHM values of 6 nm are obtained for the pattern of Fig. 5(b); while for single lines such as the one shown Fig. 1, we obtain a FWHM of about 15 nm.

The sharpest silicon oxide structure (lines and/or dots) reported in literature has a slope of 0.15 which implies for a local oxide thickness of 1 nm a linewidth of 14 nm at its base. Does a minimum baseline width of 14 nm represent an intrinsic limit in local oxidation nanolithography of silicon surfaces? The individual factors that control the feature size on silicon surfaces have been previously identified.[4,5,13,16] Chiefly among them are the meniscus size, the spatial variation of the electrical field inside the liquid meniscus, the lateral diffusion of the oxyanions, the space-charge buildup during growth, and the three dimensional character of the structures. However, it is not straightforward to separate those factors experimentally. Furthermore, a model considering the interplay of those factors is still lacking. This, in turn, makes it hard to design an experiment to go beyond the feature size limit found here. We can not dismiss the possibility of finding a clever combination of some of the aforementioned factors to obtain smaller features.

In short, we have measured the linewidth of silicon–oxide structures fabricated by local oxidation lithography and imaged by AFM. We have contemplated two different structures, isolated lines and packed structures. The structures have been fabricated in the proximity of an object of known shape and size comparable to the oxide motives. The comparison between local oxide structures and sexithiophene islands reveals that AFM images faithfully reproduce the size and shape of local silicon oxides. The oxide lines on silicon have a trapezoidal shape with a flat section at the top. The angle with the horizontal ranges between 3° and 8°. We have produced linewidths of 7 nm and 20 nm at the top and base, respectively. Shallow angles imply a minimum feature size of 14 nm for an oxide protruding 1 nm from the surface. The very same reason, shallow angles allow one to pack structures with a separation smaller than the linewidth at the base. Arrays of lines have been packed with a periodicity of 13 nm.

ACKNOWLEDGMENTS

This work was supported by the Dirección General de Enseñanza Superior e Investigación (PB98-0471) and the European Comission (MONA-LISA, G5RD-2000-00349). Sexithiophene molecules were prepared at the ISM (Bologna, Italy) by F. Biscarini and M. Murgia. The authors also acknowledge helpful discussions with M. Calleja.

[1] E. S. Snow, P. M. Campbell, F. A. Buot, D. Park, C. R. K. Marrian, and R. Magno, Appl. Phys. Lett. **72**, 3071 (1998).
[2] R. Held, T. Vancura, T. Heinzel, K. Ensslin, M. Holland, and W. Wegscheider, Appl. Phys. Lett. **73**, 262 (1998).
[3] K. Matsumoto, Y. Gotoh, T. Maeda, J. A. Dagata, and J. S. Harris, Appl. Phys. Lett. **76**, 239 (2000).
[4] R. García, M. Calleja, and H. Rohrer, J. Appl. Phys. **86**, 1898 (1999).
[5] J. A. Dagata, T. Inoue, J. Itoh, K. Matsumoto, and H. Yokoyama, J. Appl. Phys. **84**, 6891 (1998).
[6] F. S. Chien, Y.-C. Chou, T. T. Chen, W.-F. Hsieh, T. S. Chao, and S. Gwo, Appl. Phys. Lett. **89**, 2465 (2001).
[7] Y. Okada, Y. Luchi, M. Kawabe, and J. S. Harris, J. Appl. Phys. **88**, 1136 (2000).
[8] E. Dubois and J.-L. Bubendorff, J. Appl. Phys. **87**, 8148 (2000).
[9] J. Shirakashi, K. Matsumoto, N. Miura, and M. Konagai, Jpn. J. Appl. Phys., Part 2 **36**, L1257 (1997).
[10] E. Snow, P. M. Cambell, and F. K. Perkins, Proc. IEEE **85**, 601 (1997).
[11] A. Avramescu, A. Ueta, K. Uesugi, and I. Suemune, J. Appl. Phys. **88**, 3158 (2000).
[12] R. Maoz, E. Frydman, S. R. Cohen, and J. Sagiv, Adv. Mater. **12**, 725 (2000).
[13] P. Avouris, T. Hertel, and R. Martel, Appl. Phys. Lett. **71**, 285 (1997).
[14] M. Calleja and R. García, Appl. Phys. Lett. **76**, 3427 (2000).
[15] M. Tello and R. García, Appl. Phys. Lett. **79**, 424 (2001).
[16] J. A. Dagata, F. Pérez-Murano, G. Abadal, K. Morimoto, T. Inoue, J. Itoh, and H. Yokoyama, Appl. Phys. Lett. **76**, 2710 (2000).
[17] E. B. Cooper, S. R. Manalis, H. Fang, H. Dai, S. C. Minne, T. Hunt, and C. F. Quate, Appl. Phys. Lett. **75**, 3566 (1999).
[18] V. Bouchiat, M. Faucher, C. Thirion, W. Wernsdorfer, T. Fournier, and B. Pannetier, Appl. Phys. Lett. **79**, 123 (2001).
[19] F. S. Chien, C.-L. Wu, Y.-C. Chou, T. T. Chen, S. Gwo, and W.-F. Hsieh, Appl. Phys. Lett. **75**, 2429 (1999).
[20] S. C. Minne, J. D. Adams, G. Yaralioglu, S. R. Manalis, A. Atalar, and C. F. Quate, Appl. Phys. Lett. **73**, 1742 (1998).
[21] Y. Gotoh, K. Matsumoto, T. Maeda, E. B. Cooper, S. R. Manalis, H. Fang, S. C. Minne, T. Hunt, H. Dai, J. Harris, and C. F. Quate, J. Vac. Sci. Technol. A **18**, 1321 (2000).
[22] R. García and A. San Paulo, Phys. Rev. B **61**, R13381 (2000).
[23] R. García and A. San Paulo, Phys. Rev. B **60**, 4961 (1999).
[24] F. Biscarini, R. Zamboni, P. Samorí, P. Osotja, and C. Taliani, Phys. Rev. B **52**, 14868 (1995).
[25] D. Keller and F. S. Franke, Surf. Sci. **294**, 409 (1993).
[26] K. Morimoto, K. Araki, K. Yamashita, K. Motira, and M. Niwa, Appl. Surf. Sci. **117**, 652 (1997).
[27] K. Morimoto, F. Pérez-Murano, and J. Dagata, Appl. Surf. Sci. **158**, 205 (2000).